Construction and Building Materials 158 (2018) 691–699

Contents lists available at ScienceDirect

Construction and Building Materials

journal homepage: www.elsevier.com/locate/conbuildmat

Fluxing as a new tool for bitumen rheological characterization and the use of time-concentration shift factor (a_c)

Salah E. Zoorob [a], Georges A. Mturi [b], Cesare Sangiorgi [c], Marisa Dinis-Almeida [d], Noor Zainab Habib [e,*]

[a] Construction and Building Materials Program, Kuwait Institute for Scientific Research, P.O. Box 24885 Safat, 13109, Kuwait
[b] CSIR Built Environment, Transport Infrastructure Engineering, P.O. Box 395, Pretoria 0001, South Africa
[c] DICAM-Roads, Dept. of Civil, Environmental and Materials Engineering, University of Bologna, V.le Risorgimento 2, 40136 Bologna, Italy
[d] C-MADE, Centre of Materials and Building Technologies, University of Beira Interior, Calçada Fonte do Lameiro, Edifício II das Engenharia, 6200-001 Covilhã, Portugal
[e] Institute of Infrastructure and Environment, Heriot- Watt University Dubai Campus, P.O. Box 294345, Dubai, United Arab Emirates

HIGHLIGHTS

- Time-concentration an alternative tool to Time-temperature superposition.
- Fluxed bitumens enable Time-Concentration to replace Time-Temperature shifting.
- Fluxing bitumens simulative of raising test temperature.

ARTICLE INFO

Article history:
Received 7 June 2017
Received in revised form 2 October 2017
Accepted 3 October 2017
Available online 19 October 2017

Keywords:
Bitumen rheological characterization
Time-temperature superposition
Time-concentration superposition
Bitumen fluxing
Free volume shifting

ABSTRACT

The concept of temperature shift factor (a_T) as defined by Doolittle, relating the free volume of a viscoelastic material at the current and reference states is briefly examined together with the resultant William-Landel-Ferry equation. This paper highlights the fact that change in free volume arise not only from temperature variations but can also result from the absorption of solvents and thus a generalized Doolittle relation may also be applied to a solvent concentration shift factor (a_c). To validate this concept, a small scale laboratory investigation was carried out by blending 40/60 penetration grade bitumen with various proportions of one type of cooking oil and conducting dynamic shear rheometer frequency sweeps at a range of temperatures. By applying time-concentration superposition to each flux content, it was possible to shift horizontally (a_c) each set of complex modulus data measured at each test temperature, so that all sets superimpose onto the master curve of the base bitumen at a preselected reference temperature. A direct relationship between conventional time-temperature shift and the proposed time-concentration shift factors was thus demonstrated using a sample of penetration grade bitumen and one type of vegetable oil. Further experimentation with other bitumen-flux combinations is necessary prior to recommending general adoption of the proposed tool.

1. Introduction

1.1. Background of study

1.1.1. Introduction to bitumen fluxing

It is widely accepted that bitumens are miscible with each other to form homogeneous blends in all proportions, though care must be exercised when blending a penetration grade bitumen with a blown oxidised bitumen. Bitumens can also be blended with a wide variety of crude oil-based fractions depending on the application. Volatile light fractions (e.g. white spirit) are used when rapid curing is required; less volatile fractions (e.g. kerosene) are used for longer drying times as for cutback bitumens [15].

Bitumen preparations where the viscosity of the binder has been reduced by the addition of relatively non-volatile oils are referred to as fluxed bitumens. The added oil is known as a fluxing agent or fluxant that is typically gas oil, vegetable based oils [5,10], or methyl esters of fatty acids [13,16].

When designing reclaimed asphalt pavement (RAP) mixes, it is popular to utilize bitumen blending charts similar to that shown in Fig. 1, [2,24]. The viscosity of the aged bitumen in the RAP is plotted on the left hand vertical scale (Point A). A vertical line repre-

* Corresponding author.
E-mail addresses: szoorob@kisr.edu.kw (S.E. Zoorob), GMturi@csir.co.za (G.A. Mturi), cesare.sangiorgi4@unibo.it (C. Sangiorgi), marisa.dinis@ubi.pt (M. Dinis-Almeida), n.habib@hw.ac.uk (N.Z. Habib).

https://doi.org/10.1016/j.conbuildmat.2017.10.020
0950-0618/

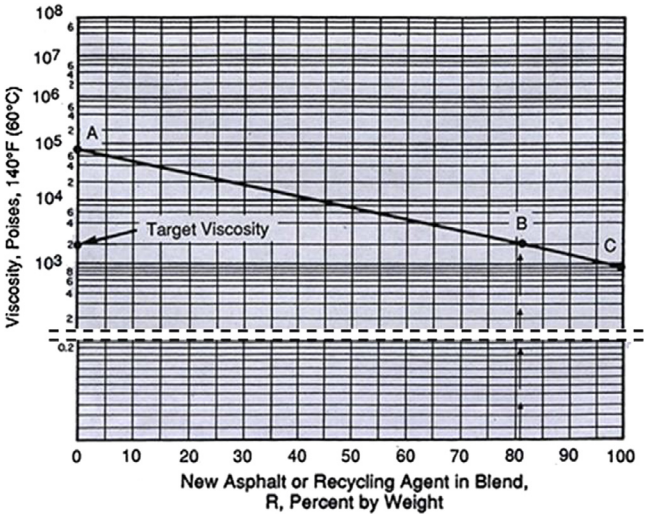

Fig. 1. Bitumen blending chart [24].

senting the percentage of new bitumen required (R) is drawn and its intersection (Point B) with the horizontal line representing the target viscosity is determined. A straight line from Point A, through Point B is next extended to intersect the right hand scale. Point C is the viscosity of the new bitumen (and/or recycling agent) required to blend with the bitumen in the RAP to obtain the target viscosity in the blend. Note that the y axis in Fig. 1 is a double log scale (Walther function), thus resulting in an accuracy level which may be described as "approximate". More recent work on rejuvenating RAP using bio-materials can also be found in [7].

There is abundant evidence and theoretical justification in the polymer science literature highlighting the fact that when a polymer is diluted (fluxed) with a solvent with which it forms a true solution, the viscosity of the blend is reduced [12]. The primary objective of this paper is to simply demonstrate the feasibility of transferring both the theoretical arguments and interpretation techniques from fluxing polymers across to the bitumen field. In the following sections the theoretical background and justification is first introduced followed by a limited experimental proof of concept utilizing a single type of bitumen fluxed with one type of vegetable oil.

1.1.2. Models for blended binders

A number of relationships exist for estimating the penetration and softening point of a bitumen blend. As an example, the Shell Bitumen Handbook recommends the following two formulae [15]:

$$\log P = \frac{A \log P_a + B \log P_b}{100} \tag{1}$$

where: P = penetration of the final blend, P_a = penetration of component 'a', P_b = penetration of component 'b', A = % of component 'a' in the blend, B = % of component 'b' in the blend.

$$S = \frac{A\ S_a + B\ S_b}{100} \tag{2}$$

where: S = softening point of the final blend, S_a = the softening point of component 'a', S_b = softening point of component 'b', A = % of component 'a' in the blend, B = % of component 'b' in the blend.

It is interesting to note that Eq. (1) is likely derived from early work conducted by Arrhenius to predict the steady state viscosity (η_0) of ideal binary mixtures of mineral oils [8]:

$$\ln \eta_0 = \frac{V_1}{V} ln\ \eta_1 + \frac{V_2}{V} ln\ \eta_2 \tag{3}$$

where: η_1 and η_2 = the viscosities of the component oils, V_1 and V_2 = volumes of the oils making up the blend, V = volume of the blend.

Another method worthy of mentioning is the Refutas viscosity blending function which was developed to predict blend viscosities of all petroleum components from gasoline to vacuum residue [6]. In this method a Viscosity Blending Index (VBI) of each component is first calculated and then used to determine the VBI of the liquid mixture as shown below.

$$VBI_i = 14.534 \times ln(ln(\upsilon_i + 0.8)) + 10.975 \tag{4}$$

where: v_i = kinematic viscosity in centistokes (cSt). It is important that the kinematic viscosity of each component of the blend be obtained at the same temperature.

The VBI of the liquid mixture is then calculated as follows:

$$VBI_{mixture} = \sum_{i=1}^{N} (x_i \times VBI_i) \tag{5}$$

where: x_i = the mass fraction of component "i" of the blend; N = the number of components.

The kinematic viscosity of the mixture can then be estimated using the viscosity blending number of the mixture using the equation below.

$$\upsilon_{mixture} = exp\left(exp\left(\frac{VBI_{mixture} - 10.975}{14.534}\right)\right) - 0.8 \tag{6}$$

[22] conducted a thorough review and investigation on bitumen blending. The change in complex shear modulus (G^*) of various blends of laboratory aged and unaged binders, also blended with various proportions of recycling agents were studied at high and intermediate pavement temperatures with a Dynamic Shear Rheometer (DSR). The study demonstrated that linear relationships for shear modulus (G^*) of the blended binders can be represented numerically as follows:

$$Log\ G^*_{Blend} = LogG^*_{Aged} - X.Log\left(\frac{G^*_{Aged}}{G^*_{Recycling\ \ Agent}}\right) \tag{7}$$

where: X = proportion of recycling agent by total weight in the blend.

1.2. Background to the free volume model and the WLF equation

The free volume model is based on the assumption that the mechanical response of a viscoelastic polymer is dependent on the ability of its molecular chains to accommodate applied deformations. Free volume may be visualized as the volume that is not occupied by the molecular chains in a material that can be considered an indicator of molecular segmental mobility, where greater free volume provides the extra mobility needed to accommodate applied deformations rapidly [19].

According to the free volume theory, the glass transition temperature (T_g) represents the temperature that polymers have a certain universal free volume which controls the molecular mobility. In polymer science, T_g is also described as the point, or narrow region, on the temperature scale where the thermal expansion coefficient undergoes a discontinuity and below which the configurational rearrangements of polymer chain backbones are extremely slow [12]. The internal mobility of the system (expressed as viscosity) can be related to the fractional free volume empirically by the Doolittle viscosity Eq. (8). Eq. (8) then provides the starting point to derive the William-Landel-Ferry (WLF) equation from the free volume theory [14].

$$\eta = A.exp\left(\frac{B}{f}\right) \tag{8}$$

where: η = viscosity, A and B are constants, and f is the fractional free volume.

Doolittle defined a temperature shift factor (a_T) relating the free volume of a material at the current and reference states through the expression:

$$a_T = \frac{exp\left(\frac{B}{f}\right)}{exp\left(\frac{B}{f_r}\right)} = exp\left(B\left(\frac{1}{f} - \frac{1}{f_r}\right)\right) \quad (9)$$

where: f = fractional free volume at temperature T, and f_r = the fractional free volume at the reference temperature T_r.

The fractional free volume at temperature T can be expressed as:

$$f = f_r + \alpha_f(T - T_r) \quad (10)$$

where: α_f = the coefficient of expansion of the fractional free volume. Insertion of Eq. (10) into Eq. (9) gives:

$$a_T = exp\left(B\left(\frac{1}{f_r + \alpha_f(T - T_r)} - \frac{1}{f_r}\right)\right)$$
$$= exp\left(B\left(\frac{-\alpha_f(T - T_r)}{f_r(f_r + \alpha_f(T - T_r))}\right)\right)$$

$$= exp\left(-\frac{B}{f_r}\left(\frac{\alpha_f(T - T_r)}{f_r + \alpha_f(T - T_r)}\right)\right) = exp\left(\frac{\left[-\frac{B}{f_r}\right](T - T_r)}{\left[\frac{f_r}{\alpha_f}\right] + (T - T_r)}\right) \quad (11)$$

The following expression can be obtained by taking the logarithm of Eq. (11) [14]:

$$\log a_T = \frac{\left[\frac{-B}{2.303 f_r}\right](T - T_r)}{\left[\frac{f_r}{\alpha_f}\right] + (T - T_r)} \quad (12)$$

The WLF equation, expressed in general terms has the following form:

$$\log a_T = \frac{-C_1(T - T_r)}{C_2 + (T - T_r)} \quad (13)$$

where: $a_T = \eta_T/\eta_{Tr} = \tau_T/\tau_{Tr}$, (η represents the viscosity and τ represents a characteristic segmental relaxation time at temperatures T and T_r, C_1 and C_2 are constants). When the reference temperature T_r is set equal to the glass transition temperature (T_g), C_1 and C_2 have been found to be almost universal constants for a wide range of polymers ($C_1 = -17.44$ and $C_2 = 51.6$ K).

The WLF can equally be rewritten in natural log terms:

$$\frac{-1}{ln(a_T)} = \frac{C_2 + (T - T_r)}{C_1(T - T_r)} = \frac{C_2}{C_1(T - T_r)} + \frac{1}{C_1} \quad (14)$$

The WLF can also be rearranged to obtain the universal constants C_1 and C_2 from a linear graphical plot as follows:

$$\frac{(T - T_r)}{log\ a_T} = \frac{-(T - T_r)}{C_1} - \frac{C_2}{C_1} \quad (15)$$

1.3. Introducing the generalized shift factor

The free volume change of viscoelastic polymers has been typically associated with thermal changes and resulted in the time-temperature trade-off during material characterization. However, this change in free volume can also arise from solvent absorption and/or from mechanical stress as studied through the influence of pressure on the glass transition temperature [9].

It has thus been argued that temperature, solvent (or plasticizer or flux) concentration and mechanical dilation all influence the time scale, and hence the fractional free volume, of the material in a similar manner. The fractional free volume can be expressed as [19]:

$$f = f_0 + A \cdot \alpha(t) \cdot dT + B \cdot M(t) \cdot \sigma_{kk} + C \cdot \gamma(t) \cdot dc \quad (16)$$

Where; f_0 = the fractional free volume at an arbitrary reference temperature T_0, α(t) and γ(t) are the volume coefficients of thermal and solvent expansion respectively. In general, α(t) and γ(t) are functions of temperature (T), solvent concentration (c), the creep compliance M(t) is a function of mechanical dilation θ(t), σ_{kk} is the first stress invariant, and A, B, C are constants to be determined.

For small changes in variables below the glass transition temperature of the polymer and the boiling point of the penetrant, it may be assumed that α(t), γ(t) and M(t) are constants with respect to time. Under such conditions, Eq. (16) can be reduced to [19]:

$$f = f_0 + \alpha\Delta T + \gamma\Delta c + \delta\theta \quad (17)$$

where: $\theta = \varepsilon_{kk}$ the first strain invariant, and δ is a material constant.

Hence the shift factor a(T,c,θ) can be expressed as a function of temperature (T), solvent concentration (c) and mechanical dilation (θ). Substituting Eq. (17) into Eq. (9) gives the nonlinear shift factor [19]:

$$\text{Log } a(T, c, \theta) = -\frac{B}{2.303 f_o}\frac{\alpha\Delta T + \Upsilon\Delta C + \delta\theta}{f_o + \alpha\Delta T + \Upsilon\Delta c + \delta\theta} \quad (18)$$

For negligible solvent concentrations and dilation, Eq. (18) reduces to the WLF Eqs. (13) or (14).

There is also a correction that may be applied in the vertical direction (i.e. parallel to the y axis) along with the shift in the x axis. The temperature-dependent, vertical shift factor b_T is usually defined as the ratio of stress determined at temperature T to a "reduced stress" that is the value at a "reference temperature" T_0. The assumption that stress magnitudes, e.g. G(t), G'(ω) and G"(ω), are proportional to the product of the density and temperature implies that the vertical shift factor $b_T(T)$ has the following form [21]:

$$b_T = (T_o \times \rho_o)/(T \times \rho) \quad (19)$$

This vertical correction is invalid for the glassy state and can only be made for the rubbery state (above T_g). The value of b_T is normally close to unity as the dependence of sample density on temperature is relatively small.

1.4. Justifying the use of concentration shift factor a_c

In this section we will ignore the effects of temperature and mechanical dilation and focus on the influence of adding a non-volatile solvent (or flux or plasticizer) to our binder at constant temperature and assuming no dilation effects.

A generalized Doolittle relation can thus be applied to the concentration shift factor (ac) as follows [21].

It is worth noting that Eq. (20) is comparable to Eq. (9).

$$a_c = exp\left(D\left(\frac{1}{f} - \frac{1}{f_r}\right)\right) \quad (20)$$

where: f = fraction of free volume of the plasticized binder, f_r = fraction of free volume of the pure binder. The parameter D is assumed to be independent of molar mass, temperature and concentration. The parameter f is defined below (comparable to Eq. (10))

$$f = f_r + \beta w_1 \quad (21)$$

where: w_1 = the weight fraction of the additive, β = the pertinent parameter relating free volume to weight fraction of additive. The parameter β is in essence a measure of the molar plasticizing activity of an additive.

Further manipulation of the Eqs. (20) and (21) yields the following equation [21].

$$\frac{-1}{ln\ a_c} = \frac{f_r}{D} + \left[\frac{f_r^2}{D\beta} \times \frac{1}{w_1}\right] = \frac{C_{22}}{C_{11}(w_1)} + \frac{1}{C_{11}} \quad (22)$$

Eq. (22) is essentially comparable to Eq. (14), where a_T is equivalent to a_c, (T_r–T) is equivalent to w_1, C_1 is equivalent to C_{11} and C_2 is equivalent to C_{22}. Eq. (22) can also be rearranged and expressed in a similar manner to Eq. (15) as follows:

$$\frac{w_1}{log\ a_c} = \frac{-w_1}{C_{11}} - \frac{C_{22}}{C_{11}} \quad (23)$$

2. Materials and testing methods

In this investigation, a sample of Shell 40/60 penetration grade bitumen pen. = 56 dmm, S.P. = 50.4 °C Kuwaiti crude was blended with vegetable oil to produce a range of bitumen/oil blends. Groundnut also known as Peanut cooking oil, readily available from most supermarkets in the UK, was arbitrarily selected and used in this investigation. Typical groundnut oil characteristics based on extensive literature by [23] and [17] are as follows: Fatty Acid content = 0.05%, Iodine Value = 95.23 (g of I_2/100 g of oil), Peroxide value = 6.82 (meg/kg oil), and Anisidine value = 5.22. Typical fatty acid distribution is as follows: Saturated fatty acid (mainly Palmitic and Stearic acid) = 22.5%, Mono-unsaturated fatty acid (primarily Oleic acid) = 50.1%, Poly-unsaturated acid (primarily Linolenic acid) = 27.4%.

In the first part of the investigation, bitumen/oil blends were produced one blend at a time. The production sequence started by heating the 40/60 penetration grade to a temperature of 160 °C in an oven, transferring the bitumen tin on to a hot plate, and adding the required amount of preheated vegetable oil whilst continuously stirring each blend manually for 10 min using a kitchen whisker. To minimize the extent of vegetable oil oxidation, for each blend, approximately 0.5 L of oil was placed in a capped small glass bottle in a preheated oven set at 160 °C for 30 min and a fresh sample of oil was used for each blend. Six samples of bitumen/oil blends were produced at 0, 2, 4, 6, 8 and 10% oil contents by mass. As expected, the vegetable oil blended readily with the bitumen and there was a noticeable increase in fluidity/workability as the oil content was increased.

The 40/60 penetration grade and the various blends were also subjected consecutively to the rolling thin film oven test (RTFOT) [3] and pressure ageing vessel (PAV at 110 °C) [4] laboratory ageing protocols. For every blend at each ageing condition, i.e. Virgin, RTFOT, RTFOR + PAV, dynamic shear rheometer (DSR) test samples were cast into (8 mm and 25 mm diameter) silicon moulds (3 samples each size).

Oscillatory tests were undertaken by means of a Malvern Kinexus model DSR in strain control mode of loading using parallel plate geometry in accordance with [1]. The temperature range from 0 to 40 °C (in steps of 5 °C) was investigated using an 8 mm diameter plate (2 mm gap), whilst the range from 45 to 75 °C (in steps of 5 °C) was investigated using a 25 mm diameter plate (1 mm gap). Strain sweeps were initially conducted (results not shown in this paper) to establish the linear viscoelastic limits for base bitumen at the various test temperatures. Subsequently, at each test temperature, a frequency sweep was conducted (0.1–10 Hz) at a strain amplitude of 0.5%, well within the linear viscoelastic limit of the hardest sample tested in this investigation.

3. Results and discussion

Fig. 2 shows complex modulus (G*) versus frequency (0.1–10 Hz) individual curves obtained from DSR frequency sweeps of the 40/60 penetration grade bitumen at each test temperature (0–75 °C). Also presented is the master curve obtained by shifting the individual iso-thermal curves across the frequency axis, using the time-temperature superposition (TTS) principle, to a reference temperature T_r of 25 °C. The combined G* master curve thus extends over a much wider frequency range. TTS analysis and the generation of shift factors was carried out on the raw DSR data with the aid of proprietary software (rSpace™) pre-installed by Malvern on the Kinexus DSR. In essence the software carries out non-linear regression analysis on the rheological data. A thorough explanation of the background and comparison of various procedures for TTS, shift factors and the production of master curves can be found in Chapter 11 of [12] and [25].

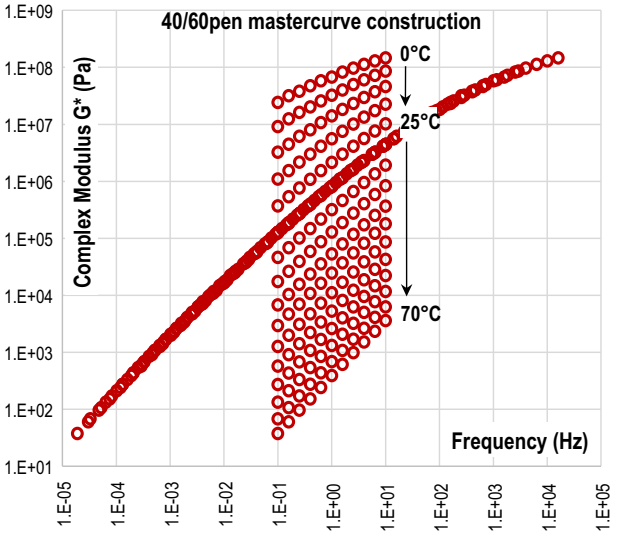

Fig. 2. Individual DSR frequency sweep curves of unaged 40/60 pen base bitumen (0–75 °C) and the master curve at 25 °C.

The same TTS procedure was repeated for each bitumen/oil blend and the results of the G* master curves (at a reference temperature of 25 °C) are shown in Fig. 3. All the G* master curves show the characteristic 45° asymptote at low frequencies (high temperatures), and they all tend in a smooth transition towards a common limiting stiffness value (glassy G*) at the upper end of the frequency (lower temperature) spectrum.

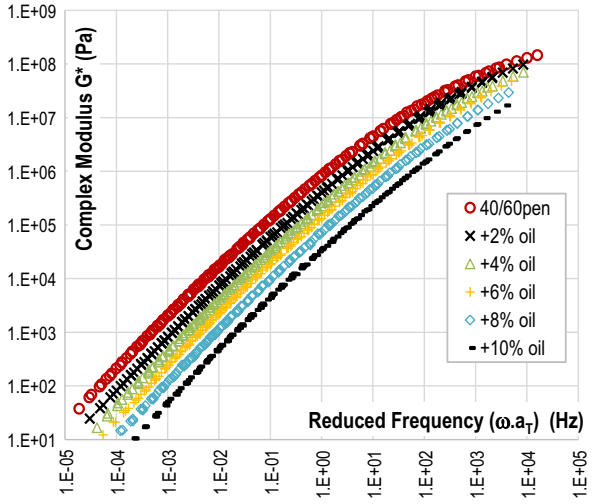

Fig. 3. G* master curves (all at 25 °C) of the base bitumen and all unaged bitumen-oil blends.

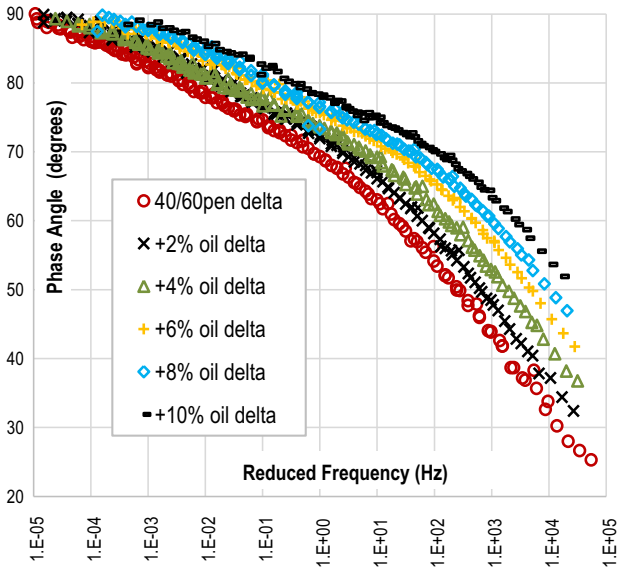

Fig. 4. Phase angle (δ) master curves (25 °C) of the unaged base bitumen and bitumen-oil blends.

Fig. 4 shows the results of the TTS principle having been applied to the phase angle (δ) results to generate δ master curves also at 25 °C. Observing either Fig. 3 or Fig. 4, one notices that the G* or δ master curves of the various blends have high resemblance with respect to shape and presented merely simple horizontal shifts (translations) of the 40/60pen master curve across the frequency axis. Simple visual interpretation of the G* or δ master curves indicates that vegetable oil blending has not introduced any visibly obvious rheologic modifications to the base bitumen (e.g. major changes in slope, curvature, or discontinuities) beyond what is expected from a chemically compatible non-interactive flux (i.e. simple reduction in viscosity), though this requires further quantitative verification with the aid of optimization techniques.

To emphasise the point that the various binder curves are merely horizontal translations, Fig. 5 shows the 10% oil blend G* master curve superimposed on the control 40/60pen G* master curve (all at 25 °C), and the two curves in Fig. 5 are almost inseparable.

In Fig. 6, the relationship between G* and δ over the entire temperature and frequency range are presented in the form of Black diagram curves for two binder types, i.e. the base 40/60pen bitumen and the 6% oil-bitumen blend. The advantage of plotting Black diagrams is that for each binder type, the raw G* and δ data at all test temperatures can be simply visualized in their original (un-shifted) form. Simple visual observation shows that the 6% oil blend (un-shifted frequency sweep data) superimposes on the thermo-rheologically simple 40/60pen base bitumen curve with a reasonably good fit. Identical behaviour was observed for the 2% and 4% oil blends.

Beyond 6% oil addition, the assumption of rheogical "simplicity" appears to become gradually less credible. The example shown in Fig. 7 is a Black diagram showing the 10% oil blend superimposed onto the 40/60 pen base bitumen curve. It is clear in Fig. 7 that the compatibility or peptizing ability of the vegetable oil in the bitumen becomes more questionable beyond 6%. Utilizing black diagrams is a very effective technique to ensure compatibility (absence of phase separation) of the various blend components. Relying on the goodness of fit of superimposed (shifted) G* curves, as shown earlier in Fig. 5 as an example, would not have revealed the lack of compatibility issue at 10% oil content.

The potential for superimposing Black diagrams of various binders was also assessed using RTOFT + PAV conditioned samples. Fig. 8 presents the Black diagrams for the 40/60pen virgin, 40/60pen aged and 6% oil-bitumen blend/aged binders. As expected, aged binders had lower phase angle values (to the left side) of the unaged 40/60pen. Simple visual observation of the goodness of fit of the superimposed 6% oil-bitumen aged blend onto the aged 40/60pen shown in Fig. 8 was not as good as was the case for the virgin binders (Fig. 6). This can be attributed to the fact that due to the completely different chemical composition, vegetable oils age at a different rate compared to petroleum derived bituminous binders. The triacylglycerol structure, which forms the backbone of most vegetable oils are associated with different fatty acid chains. The presence of unsaturation in the triacylglycerol molecule e.g. due to C=C from oleic, linoleic, and linolenic acid moieties, functions as the active sites for various oxidation reactions [11,16]. Once again a simple visual assessment shows

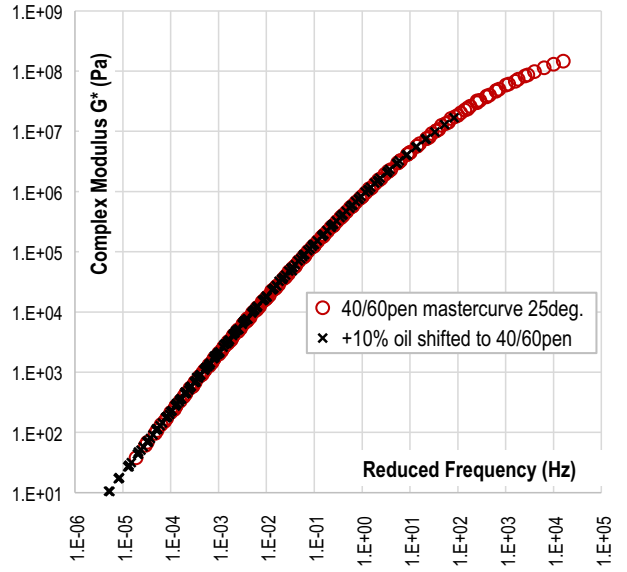

Fig. 5. G* master curve of the unaged 10% oil-bitumen blend superimposed onto the unaged base 40/60pen G* master curve at 25 °C.

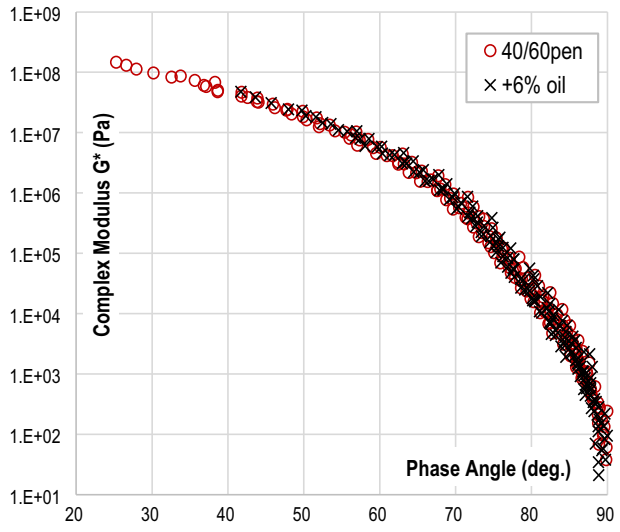

Fig. 6. G* versus δ data from frequency sweeps of the unaged base 40/60pen and 6% oil-bitumen blend.

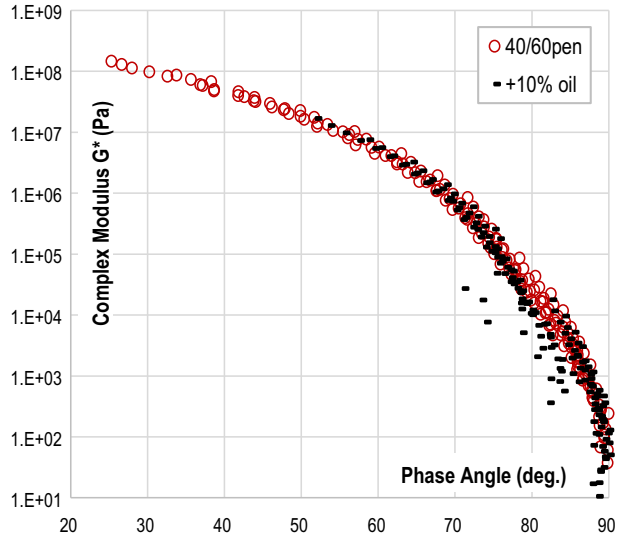

Fig. 7. G^* versus δ data from frequency sweeps of the unaged base 40/60pen and 10% oil-bitumen blend.

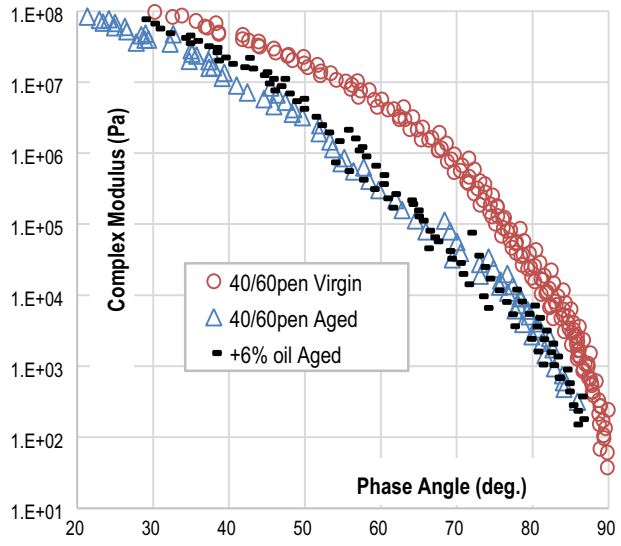

Fig. 8. Black diagrams of the 40/60pen base bitumen, 40/60pen RTROT + PAV aged, and 6% oil-bitumen RTFOT + PAV aged binders.

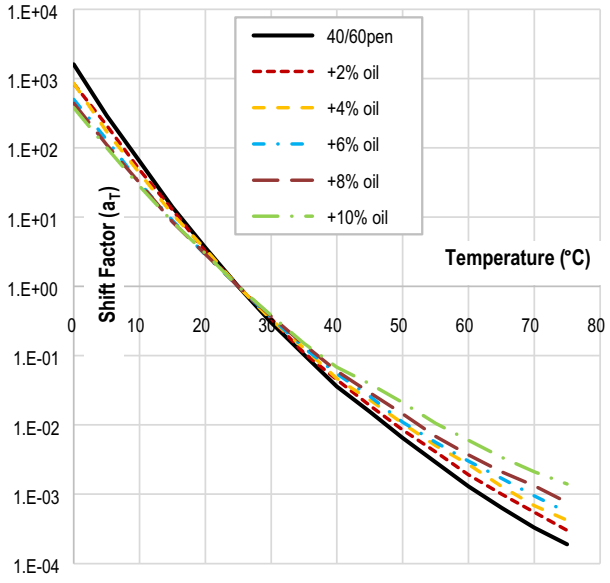

Fig. 9. TTS shift factors (a_T) for the base bitumen and all other oil-bitumen blends, to produce master curves for each binder type at 25 °C.

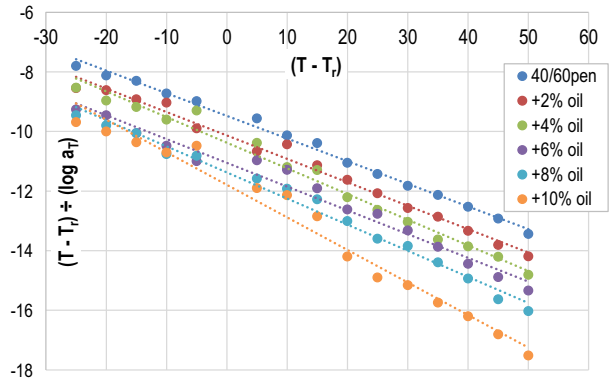

Fig. 10. Graphical representation of the WLF equation for each of the binders tested in this investigation.

that the goodness of fit of the Black diagrams of the aged binders deteriorates rapidly above 6% oil content.

Fig. 9 presents the time-temperature shift (TTS) factors (a_T) for each of the base bitumen and the five unaged blends investigated. The a_T values shown indicate the amount of horizontal shifting (across the frequency axis) that must be applied to each binder type at each test temperature to generate master curves at 25 °C. It is interesting to note that overall, the amount of shifting required at any one temperature reduces progressively as the oil content increases (softer binder).

Each line in Fig. 10 is a graphical presentation of the WLF Eq. (15) for a particular binder at the reference temperature T_r of 25 °C. The slope of each line is equivalent to $(-1/C_1)$ and the intercept with the y axis at $(T–T_r = 0)$ represents the constant $(-C_2/C_1)$. The values of the constants C_1 and C_2 for each binder blend is presented in Table 1. Using these constants, for each binder type, it would be possible to determine the amount of horizontal shift (a_T), across the frequency axis, required for a set of G^* data acquired at any test temperature (T) to form a master curve of that binder at the reference temperature (T_r) of 25 °C.

Table 1
Values of the WLF constants C_1 and C_2 for all binder blends investigated (reference temperature = 25 °C).

Binder type	WLF constant C_1	WLF constant C_2
40/60pen	30.29	124.69
40/60pen + 2% oil	29.29	128.91
40/60pen + 4% oil	26.71	120.34
40/60pen + 6% oil	28.89	138.61
40/60pen + 8% oil	26.28	129.81
40/60pen + 10% oil	21.08	107.93

Next, using the concept of time-concentration superposition, for each flux content, it is possible to shift horizontally each of the sets of G^* data measured at any test temperature, so that all sets individually superimpose on to the master curve of the 40/60pen base bitumen at 25 °C. An example of the 10% oil raw data and the concentration-shifted data is shown in Fig. 11.

Using the analogy of polymer dilution with a solvent, the following corresponding explanations may be proposed regarding the physical effects of fluxing on bitumens. When a polymer is

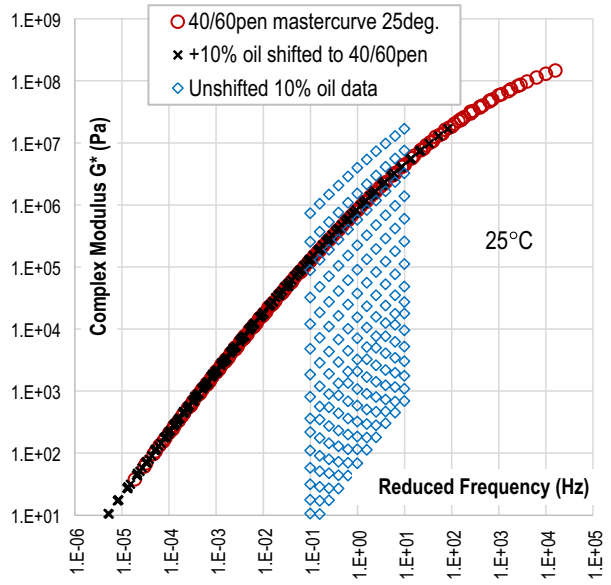

Fig. 11. A graphical representation of shifting 10% oil-bitumen blend individual frequency sweep curves (obtained at different temperatures) to superimpose on to the 40/60pen base bitumen master curve at 25 °C. The amount of shifting required at each temperature represents the concentration shift factors (a_c).

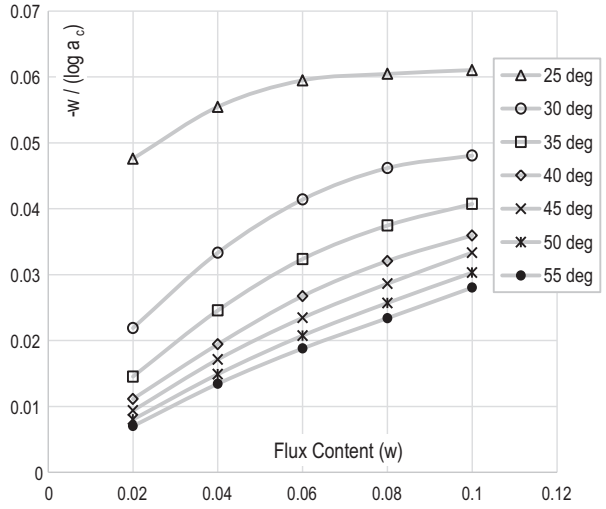

Fig. 12. Ratio of added flux by mass to log of concentration shift factors (a_c) versus flux content.

diluted with a solvent of low molecular weight, with which it forms a true solution in the sense that the solvent is molecularly dispersed, the local (monomeric) friction coefficient (i.e. the resistance encountered by a sub-molecule junction moving through its surroundings) is usually sharply reduced. Each polymeric chain unit has in its vicinity diluent molecules as well as other polymeric segments, and the former can be displaced in translatory motion much more easily, thus lowering the effective local viscosity. With increasing proportion of diluent, the monomeric friction coefficient is normally diminished, as evidenced by displacement of logarithmic plots of viscoelastic functions in the transition zone to higher frequencies or shorter times with relatively little change in shape, which agrees with the limited experimental data presented in this investigation, [12,20].

Moreover, the addition of a diluent of low molecular weight depresses T_g sharply and this depression can be attributed to the introduction of additional free volume with the diluent, as would be expected if the fractional free volume of the diluent exceeds that of the polymer and the free volumes are additive. With increasing dilution of polymers, the temperature dependence of relaxation times referred to a fixed reference temperature T_r becomes less pronounced as T_g is depressed more and more below T_r and c_2 increases whiles c_1 decreases. Furthermore, plasticizing effectiveness increases rapidly as the temperature is lowered and T_g is approached causing large changes in shift factor a_c [12].

The results in Table 1 do not show a clear trend of C_1 or C_2 values increasing or otherwise with amount of fluxing, though it must be reiterated that these results are based on one bitumen grade in combination with one oil type and more work is needed.

Fig. 12 shows a plot of "ratio of added flux to the log of concentration shift factor (a_c)" versus the "proportion of added flux by mass". Each line in Fig. 12 represents a solution of Eq. (23) (which is comparable to the WLF Eq. (15)) at a specific temperature. For the sake of clarity, only the results of 25, 30, 35, 40, 45, 50, 55 °C are shown.

As an example, the second line from the top in Fig. 12, shows the amount of shifting that has to be performed across the frequency axis for a range of oil flux contents (all tested at 30 °C), to bring back their individual 30 °C G* values to the values equivalent to the G* of the base 40/60pen bitumen at the reference temperature of at 25 °C. Similarly, the third line represents the amount of shifting that needs to be carried out, if the fluxed binders are all at 35 °C, so that the G* values are equivalent to the 40/60pen master curve at 25 °C, etc.

Interestingly, the lines in Fig. 12 do not represent linear relationships and hence do not allow the direct use of Eq. (23) (by extrapolation to w = 0) for deriving the C_{11} and C_{22} constants. One possible solution would be to plot the data on a log-log scale as shown in Fig. 13, which would "straighten" the curves. Fig. 13 is one potential solution, though the use of log-log scales to artificially produce linear graphical relationships introduces a degree of inaccuracy in the procedure. There are likely to be better mathematical treatments of shift factors than the WLF equation, for example a modified form of the Kaelble shift equation [18], may allow direct use of the data shown in Fig. 12 without having to resort to double log scales, which is beyond the scope of this simplified conceptual paper.

Now going back to the original objective, which is simply attempting to link temperature shift to concentration shift. As long as the TTS relationships (Eq. (15)) are available for a particular bin-

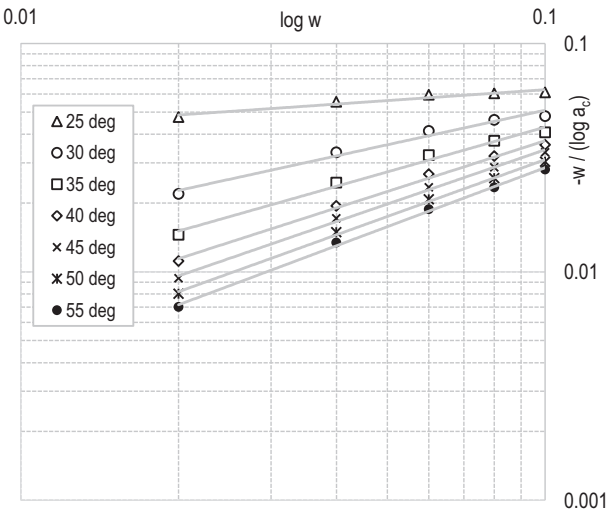

Fig. 13. Log-Log plot of the data shown in Fig. 12.

der grade, and that concentration shift data (a_c) can be produced accurately for a range of flux concentrations and a range of test temperatures, it should be possible to use the raw data directly to produce simple concentration shift charts.

Fig. 14 shows a number of a_c lines (dashed curves) versus test temperature. Each curve represents data for one flux content and all the curves shown in the Figure can be readily fitted using power law relationships of the form; $a_T = aT^b$ (where a and b are constants and T = temperature) all having R^2 values in excess of 0.99.

The solid horizontal "red" line represents an example of a temperature shift factor ($a_T = 0.0065$) for the 40/60pen to a temperature T = 50 °C from a reference temperature T_r = 25 °C. By equating a_T to a_c, we can read off from the intercept of the horizontal line with each a_c curve, the amount of flux and the test temperature that would be equal to a temperature rise of 25 °C (i.e. from 25 to 50 °C). In this example, a temperature rise of 25 °C can thus be simulated by any of the following combinations: (a) adding 2% oil to the 40/60pen and testing at 46 °C; (b) adding 4% oil and testing at 43 °C; (c) adding 6% oil and testing at 39 °C; (d) adding 8% oil and testing at 35 °C; (e) adding 10% oil and testing at 31 °C.

An alternative way of looking at the usefulness of this chart is to fix the required test temperature to a predetermined value. For example, the vertical "blue" line shown in Fig. 14 represents the reference temperature 25 °C. At 25 °C, the a_T value for the 40/60pen bitumen would be simply equal to 1. Now if we once again make $a_T = a_c$, then by adding flux to the 40/60pen, the effect becomes equivalent to increasing the test temperature. Thus, adding 2, 4, 6, 8 and 10% flux to the 40/60pen is equivalent to a_c values of 0.4, 0.2, 0.1, 0.05 and 0.02 respectively. Accepting the argument that $a_c = a_T$, the constants C_1 and C_2 for the 40/60pen from Table 1 can be input into Eq. (13), and the aforementioned a_c values become equivalent to the following temperature increments: 2.9 °C, 7.0 °C, 10.3 °C, 13.6 °C, 18.5 °C respectively.

As a further example, referring to Fig. 14, if one wishes to rheologically characterize the LVE properties of a 40/60pen (or an asphalt mix composed of the same binder) at a test temperature of (25 °C + 7 °C), one has the option of raising and maintaining the sample temperature at 32 °C, or alternatively blending 4% vegetable oil flux with the bitumen whilst maintaining the sample at the reference temperature of 25 °C.

In theory, once an accurate blending chart is established linking a_c to a_T for a particular compatible bitumen/flux system, high temperature testing can be all carried out at the same reference temperature. So for example, by fluxing the bitumen with predetermined quantities of vegetable oil, it would be possible to rapidly conduct any number of dynamic modulus tests "representing" any elevated temperature (e.g. 40, 45, 50, 55 °C, etc.) by simply conditioning all test specimens at a constant reference temperature (e.g. 25 °C). The savings in time during lengthy temperature conditioning phase for each test sample (especially if one is conducting tests at many temperatures), and the number of environmental conditioning cabinets (set at different temperatures) would be substantial. With the aid of accurate fluxing, all that would be required is the ability to condition and maintain all test samples to a single reference test temperature.

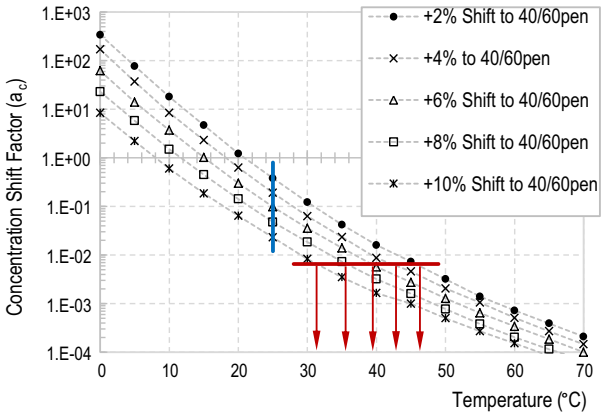

Fig. 14. Concentration shift factors for various oil/bitumen blends at various temperatures. Also shown is an example of a line equating shift factor a_T and a_c to 0.0065.

Besides the intended reduction in viscosity following fluxing, and as alluded to earlier, as long as all other rheological characteristics of the base bitumen are maintained (by fluxing only up to a predetermined limit whilst employing a compatible flux), further wider practical implications of fluxing may be envisaged. A hot mix asphalt producer may thus employ fluxing as a means of producing a range of softer grade bitumens, independently, instantaneously and whenever required, using a single source of hard bitumen. It would be easy to design an accurate fluxing/metering unit to be located immediately prior to introducing the binder to the hot aggregate mix, thus the contractor would only need a single grade of hard base bitumen and potentially a single hot bitumen storage tank, with potential for cost savings.

4. Conclusions

In summary, this paper proposes and attempts to theoretically justify a workable procedure in which time-temperature superposition as applied to penetration grade bitumen dynamic shear rheological (DSR) measurements, may be effectively replaced by time-concentration superposition. The limited laboratory investigation has demonstrated that it is possible to blend a small predetermined quantity of a non-volatile vegetable oil flux with a rheologicaly simple penetration grade base bitumen, thus affecting the rheological properties of the base bitumen to an extent equivalent to that obtained when the base bitumen temperature is increased from a reference test temperature by a fixed and quantifiable amount.

To achieve the aforementioned, the methodological steps proposed include; rheological characterization (preferably by using a DSR) of the base bitumen to produce a master curve at any selected reference temperature with the accompanying time-temperature shift factors. In the next stage, rheological data for the blending charts can be easily produced in the laboratory relating the reduction in any dynamic rheological property (complex viscosity, complex modulus, etc.) of the base bitumen to the quantity of added flux. In the final stage, by equating the time-temperature shift factors to the time-concentration shift factors, a direct correlation between temperature rise and added flux content can be achieved.

Thus at any selected reference temperature, by determining and blending an exact quantity of flux with the base bitumen, the resultant blend having reduced complex viscosity (or complex shear modulus) would accurately simulate the rheological characteristics of the base bitumen at a pre-determined higher test temperature.

The benefit of the proposed technique becomes particularly relevant when one wishes to conduct multiple LVE rheological tests (on bitumen or asphalt samples) representing a number of elevated temperatures, whilst maintaining all samples at a single reference actual test temperature. Thus the requirement for increasing the actual test temperature to simulate higher environmental temperature conditions becomes unnecessary. All that is required is a single test temperature to cover all intermediate or high temperature scenarios.

Caution must be exercised when fluxing bitumens as there is a tight limit to the amount of flux that may be added, and further-

more compatibility between the two components must be ensured. The use of Black diagram (complex modulus vs. phase angle) plots was shown to be a useful tool to assist in identifying flux proportions when blend compatibility becomes suspect.

Using the proposed methodology hot mix asphalt producers may be capable of economically producing a range of softer bitumen grades according to their needs with the aid of an accurate flux dosing mechanism and by utilizing a single harder grade base bitumen.

It must be emphasised that the hypothesis, results and analysis presented in this investigation were based on a single sample of penetration grade bitumen fluxed with a single type of vegetable oil. Further laboratory testing must be carried out on a wider range of penetration grade bitumens of different viscosities and chemistries. Extending the concept to polymer modified bitumens is beyond the scope of this investigation.

Acknowledgement

None.

References

[1] AASHTO T 315-12, Determining the Rheological Properties of Asphalt Binder Using a Dynamic Shear Rheometer (DSR), 2016.
[2] ASTM D4887/D4887M-11, Standard Practice for Preparation of Viscosity Blends for Hot Recycled Bituminous Materials.
[3] ASTM D2872-12e1, Standard Test Method for Effect of Heat and Air on a Moving Film of Asphalt (Rolling Thin-Film Oven Test).
[4] ASTM D6521-13, Standard Practice for Accelerated Aging of Asphalt Binder using a Pressurized Aging Vessel (PAV).
[5] H.K. Bailey, S.E. Zoorob, The Use of Vegetable Oil as a Rejuvenator for Asphalt Mixtures, published in 5th Eurasphalt & Eurobitume Congress, Istanbul, 2012, pp. 13–15. Also published in The UK Institute of Asphalt Technology Yearbook 2013 ISSN 1479–6341 June 2012 70 80.
[6] I. Barabás, I.A. Todoruţ, Predicting the temperature dependent viscosity of biodiesel-diesel-bioethanol blends, Energy Fuels 25 (2011) 5767–5774.
[7] A.J. Barco-Carrion, M. Perez-Martinez, A. Themeli, D.L. Presti, P. Marsac, S. Pouget, F. Hammoum, E. Chailleux, G.D. Airey, Evaluation of bio-materials rejuvenating effect on binders for high reclaimed asphalt content mixtures, Materiales de Constr. 67 (327) (2017).
[8] J. Briant, J. Denis, G. Parc, Rheological Properties of Lubricants, Institut français du pétrole publications, Éditions Technip, Paris, 1989. ISBN 2-7108-0564-2.
[9] I. Emri, W.G. Knauss, Pressure Induced Ageing of Polymers September 15-18, Third International Conference on Numerical Methods for Non-Linear Problems, Dubrovnik, Yugoslavia, 1986.
[10] Eurobitume web site, accessed 15 August 2017, http://www.eurobitume.eu/bitumen/types-bitumen.
[11] S.Z. Erhan, Vegetable oils as lubricants, hydraulic fluids, and inks, sixth ed., Wiley & Sons, 2005, pp. 259–278.
[12] J.D. Ferry, Viscoelastic Properties of Polymers ISBN 0-471-04894-1, third ed., John Wiley & Sons, 1980.
[13] I.A. Gawel, J. Pilat, P. Radziszewski, L. Niczke, J. Krol, M. Sarnowski, Bitumen fluxes of vegetable origin, Polimery 55 (1) (2010) 55–60.
[14] U.W. Gedde, Polymer Physics, Springer Science Business Media, 2013. ISBN 978-0-412-62640-1, Section 5.4.
[15] Hunter R.N., Self A., Read J., The Shell Bitumen Handbook 6th edition 2015, Appendix 3, Blending Charts and Formulae, ISBN 978-0-7277-5837-8.
[16] J.B. Król, L. Niczke, K.J. Kowalski, Towards understanding the polymerization process in bitumen bio-fluxes, Materials 1058 (2017) 10.
[17] R.D. O'Brien, Fats and Oils-Formulating and Processing for Applications, second ed., CRC Press, Boca Raton FL, USA, 2004.
[18] G.M. Rowe, M.J. Sharrock, Alternative shift factor relationship for describing the temperature dependency of the visco-elastic behaviour of asphalt materials, Trans. Res. Board 2207 (2011) 125–135.
[19] S. Roy, D. Nagendra, K.M. Liechti, Cohesive-Zone Modelling of Debond Growth at Adhesively Bonded Interfaces in Aggressive Environments Oct. 14, International Conference on Fracture (ICF10), Honolulu USA, 2001.
[20] S.P. Rwei, C.C. Lien, Synthesis and viscoelastic characterization of sulfonated chitosan solutions, Colloid Polym. Sci. 292 (2014) 785–795.
[21] A. Schausberger, I.V. Ahrer, On the time-concentration superposition of the linear viscoelastic properties of plasticized polystyrene melts using the free volume concept, Macromol. Chem. Phys. 196 (1995) 2161–2172.
[22] H.R. Soleymani, H.U. Bahia, A.T. Bergan, Blending charts based on the performance graded (pg) asphalt binder specifications, Transp. Res. Rec.: J. Transp. Res. Board 1661 (1999) 7–14. Washington D.C..
[23] C.P. Tan, Y.B. Che Man, J. Selamat, M.S.A. Yusoff, Application of arrhenius kinetics to evaluate oxidative stability in vegetable oils by isothermal differential scanning calorimetry, JAOCS 78 (11) (2001).
[24] U.S. DoT, accessed 15 June 2015, Federal Highway Administration, Pavement Recycling Guidelines for State and Local Governments, Chapter 7, Hot Mix Asphalt Recycling (Materials and Mix Design), http://www.fhwa.dot.gov/pavement/recycling/98042/07.cfm.
[25] N.I.M. Yusoff, E. Chailleux, G.D. Airey, A comparative study of the influence of shift factors on master curve construction, Int. J. Pavement Res. Technol. 4 (6) (Nov. 2011) 324–336.